OXFORD

SOT | Society of Toxicology
www.toxsci.oxfordjournals.org

TOXICOLOGICAL SCIENCES, 148(1), 2015, 121–136

doi: 10.1093/toxsci/kfv171
Advance Access Publication Date: August 6, 2015
Research Article

Incorporating High-Throughput Exposure Predictions With Dosimetry-Adjusted *In Vitro* Bioactivity to Inform Chemical Toxicity Testing

Barbara A. Wetmore,*,[1] John F. Wambaugh,† Brittany Allen,* Stephen S. Ferguson,‡,[2] Mark A. Sochaski,* R. Woodrow Setzer,† Keith A. Houck,† Cory L. Strope,* Katherine Cantwell,* Richard S. Judson,† Edward LeCluyse,* Harvey J. Clewell,* Russell S. Thomas,*,†,[3] and Melvin E. Andersen*

*The Hamner Institutes for Health Sciences, Institute for Chemical Safety Sciences, Research Triangle Park, North Carolina 27709-2137; †United States Environmental Protection Agency, Office of Research and Development, National Center for Computational Toxicology, Research Triangle Park, North Carolina 27711; and ‡Life Technologies, ADME/Tox Division of the Primary and Stem Cell Systems Business Unit, Durham, North Carolina 27703

[1]To whom correspondence should be addressed at The Hamner Institutes for Health Sciences, Institute for Chemical Safety Sciences, PO Box 12137, 6 Davis Drive, Research Triangle Park, NC 27709 Fax: (919) 558-1300. E-mail: bwetmore@thehamner.org.
[2]Present address: National Institute of Environmental Health Sciences, National Toxicology Program, Research Triangle Park, NC 27711.
[3]Present address: United States Environmental Protection Agency, Office of Research and Development, National Center for Computational Toxicology, Research Triangle Park, NC 27711.

Disclaimer: The United States Environmental Protection Agency through its Office of Research and Development reviewed and approved this publication. However, it may not necessarily reflect official Agency policy, and reference to commercial products or services does not constitute endorsement.

ABSTRACT

We previously integrated dosimetry and exposure with high-throughput screening (HTS) to enhance the utility of ToxCast HTS data by translating *in vitro* bioactivity concentrations to oral equivalent doses (OEDs) required to achieve these levels internally. These OEDs were compared against regulatory exposure estimates, providing an activity-to-exposure ratio (AER) useful for a risk-based ranking strategy. As ToxCast efforts expand (ie, Phase II) beyond food-use pesticides toward a wider chemical domain that lacks exposure and toxicity information, prediction tools become increasingly important. In this study, *in vitro* hepatic clearance and plasma protein binding were measured to estimate OEDs for a subset of Phase II chemicals. OEDs were compared against high-throughput (HT) exposure predictions generated using probabilistic modeling and Bayesian approaches generated by the U.S. Environmental Protection Agency (EPA) ExpoCast program. This approach incorporated chemical-specific use and national production volume data with biomonitoring data to inform the exposure predictions. This HT exposure modeling approach provided predictions for all Phase II chemicals assessed in this study whereas estimates from regulatory sources were available for only 7% of chemicals. Of the 163 chemicals assessed in this study, 3 or 13 chemicals possessed AERs < 1 or < 100, respectively. Diverse bioactivities across a range of assays and concentrations were also noted across the wider chemical space surveyed. The availability of HT exposure estimation and bioactivity screening tools provides an opportunity to incorporate a risk-based strategy for use in testing prioritization.

Key words: predictive toxicology; ToxCast; *in vitro-in vivo* extrapolation; dosimetry; exposure assessment

Since the release of the NRC's (2007) "Toxicity Testing in the 21st Century," governmental, academic, and industry researchers have dedicated significant research resources to generate data, make it publically accessible, and determine the utility of high-throughput (HT) and *in vitro* tools in chemical toxicity testing. The U.S. Tox21 and ToxCast research programs have leveraged HT assays developed for the pharmaceutical industry to characterize biological activities and forecast effects that may be elicited following chemical exposure (Attene-Ramos *et al.*, 2013; Dix *et al.*, 2007; Judson *et al.*, 2010; Kavlock *et al.*, 2012). Additional efforts are underway to assess *in vitro* strategies that identify toxicity pathways most relevant for industrial chemicals and to determine the concentrations at which perturbations and adverse effects are likely to arise (Adeleye *et al.*, 2015; Landesmann *et al.*, 2013; Mennecozzi, 2012). These *in vitro* testing efforts are complemented by bioinformatic and data visualization tools that have emerged from high-throughput screening (HTS) and genomics research efforts (McMullen *et al.*, 2014; Pastrello *et al.*, 2014; Pleil *et al.*, 2011; Reif *et al.*, 2013). Although the maturation and refinement of these *in vitro* and HT testing tools are promising for EPA decision-making, these tools are limited to providing hazard-based assessments. The lack of exposure information makes use in risk-based assessments difficult.

To be useful in the emerging next generation of risk science (Krewski *et al.*, 2014), dosimetry-adjusted *in vitro* bioactivity data (Rotroff *et al.*, 2010b; Wetmore *et al.*, 2012) will need to be framed in the context of human exposure. This context will inform whether concentrations eliciting activity in the bioassays will be encountered in relevant *in vivo* chemical exposure scenarios. Development of a HT exposure estimation strategy will complement data obtained from HT testing programs such as ToxCast. Published HT exposure modeling tools have been largely limited to assessing chemical fate and transport from far field sources (Arnot *et al.*, 2006; Rosenbaum, 2008). Although an important first step, HT modeling tools that capture both far- and near-field sources of chemical exposure are necessary to provide a more realistic estimate of daily human exposures.

In this report, we describe the first attempt to incorporate HT chemical toxicity testing data with HT predictions of exposure to provide a rapid, risk-based prioritization approach. *In vitro* assays measuring hepatic clearance and plasma protein binding conducted on ToxCast Phase II chemicals parameterize a pharmacokinetic (PK) model based upon *in vitro-in vivo* extrapolation (IVIVE). This model was used to predict the chemical steady-state concentrations (C_{ss}) in plasma resulting from repeated daily exposure (Rotroff *et al.*, 2010b; Wetmore *et al.*, 2012). Reverse dosimetry (Tan *et al.*, 2007) tools were then used to estimate the oral equivalent dose (OED), in mg/kg/day, required to achieve blood C_{ss} levels identical to the activity concentrations (eg, AC_{50}) in the ToxCast assays. These OEDs were then compared against exposures from a probabilistic prediction tool developed by the USEPA ExpoCast program. This tool utilizes chemical-specific use and production data that have been found to correlate with chemical exposures inferred from urinary analyte (exposure biomonitoring) data from the Center for Disease Control's (CDC's) National Health and Nutrition Examination Survey (NHANES). The NHANES characterizes central tendencies (ie, geometric means) of chemical exposures for populations in the United States (Calafat, 2012). Bayesian modeling is used to both account for unknown information that is needed to predict exposures while also quantifying the uncertainty of the predicted geometric means (Wambaugh *et al.*, 2014). Comparison of the OEDs to these exposure predictions, both expressed in mg/kg/day, provides a useful first-order approximation of activity-to-exposure ratios (AERs)—in essence a margin of exposure (MOE)—that can help shift from a hazard-centric approach toward a more risk-based strategy that can inform prioritization strategies (Thomas *et al.*, 2013).

MATERIALS AND METHODS

Chemical selection and stock preparation. The 178 ToxCast Phase II chemicals (http://www.epa.gov/ncct/toxcast/chemicals.html) [last accessed August 20, 2015] analyzed in this study were selected based on the existence of an analytical chemistry detection method and the availability of human exposure data. Compounds for the plasma protein binding and metabolic stability assays were obtained from Compound Focus, Inc (Evotec, South San Francisco, California) in neat form. Dimethyl sulfoxide (DMSO) stock solutions were prepared from the neat chemicals to generate the analytical calibration curves and for use in the assays. All stock solutions were stored at $< -70^{\circ}C$. Specific vendor and vendor-supplied purity information for each chemical is provided as Supplementary material (Supplementary Table S1).

Plasma protein binding assay. Plasma protein binding was measured for each chemical using either the rapid equilibrium dialysis (RED) method as described previously (Rotroff *et al.*, 2010b; Waters *et al.*, 2008; Wetmore *et al.*, 2012) or ultrafiltration as described later. The human plasma used in the assay was obtained from healthy, consented, paid donors at a U.S. Food and Drug Administration-licensed and inspected donor center (#HMPLEDTA2; Bioreclamation, Inc, Westbury, New York). The plasma was pooled from 5 male (37, 22, 27, 36, and 21 years old) and 5 female (30, 40, 47, 55, and 54 years old) adults and stored at $< -70^{\circ}C$ until use.

Determination of plasma protein binding by ultrafiltration was conducted on a subset of chemicals for which equilibrium dialysis resulted in unbound values $\geq 100\%$. This phenomenon has been observed with a subset of ToxCast industrial chemicals (eg, plasticizers, phthalates) and is believed to occur due to binding and/or interactions with dialysis plate components (data not shown). Briefly, plasma was thawed to room temperature and, if necessary, pH adjusted to 7.4. DMSO stocks of chemicals (200X) were added to plasma to achieve a final concentration of 10 μM. Samples were vortexed and incubated at 37°C in a water bath in polypropylene tubes prior to centrifugation in a Centrifree ultrafiltration device (Millipore Cat No. 4104, Billerica, Massachusetts) at 2000 × g for 20 min at 37°C. Ultrafiltrates were collected for analysis. This procedure ensured that the ultrafiltrate did not exceed 40% of the initial volume and minimized dissociation of bound compound due to removal of free compound (Whitlam and Brown, 1981). Nonspecific binding (NSB) was measured in a similar manner, with chemical stocks added to phosphate-buffered saline, pH 7.4 to achieve a final concentration of 10 μM, incubated at 37°C, and aliquots collected from both the preCentrifree device incubation and the post-centrifugation ultrafiltrate. All samples were run in triplicate and stored at $< -70^{\circ}C$ prior to analysis.

Metabolic clearance assay. Hepatic clearance was measured using the substrate depletion method (Wetmore *et al.*, 2012). Chemicals at 2 concentrations (1 and 10 μM) were incubated over a 240 min period with pooled cryopreserved primary human hepatocytes (Life Technologies; Durham, North Carolina). The pool of cryopreserved hepatocytes was

comprised of 14 individual adult donors of mixed gender and ethnicity (6 male Caucasians and 1 male African American; 6 female Caucasians and 1 female African American.) The hepatocytes were characterized for metabolism (CYPs 1A2, 2B6, 2C8, 2C9, 2C19, 2D6, 2E1, 3A4/5, and flavin-containing monooxygenases (FMOs)) and viability (Trypan Blue exclusion). Lot values fell within acceptable ranges compared with historical quality control limits. See Supplementary Table S1B for the metabolic characterization data. The human hepatocytes were obtained under a protocol that was reviewed and approved by an Institutional Review Board and operated in accordance with Federal Regulation for the protection of human research subjects.

Three of the chemicals for which *in vivo* PK data were available showed no loss from the hepatocyte suspensions. These were also assessed for clearance using plated hepatocytes over a 48-h time course (0, 4, 8, 24, and 48 h) at the 1 μM chemical concentration (Smith *et al.*, 2012). Plateable cryopreserved human hepatocytes (Triangle Research Laboratories, Research Triangle Park, North Carolina) were obtained from 2 adult donors under an approved Institutional Review Board (IRB) protocol and were characterized for metabolism and viability. The donor-derived hepatocytes were run individually (ie, not pooled). Hepatocyte maintenance medium (LifeTechnologies Corporation, Durham, North Carolina) supplemented with an insulin-transferrin-selenium (ITS+) supplement, dexamethasone, and penicillin/streptomycin (no serum) was utilized, with a final density of 48 000 cells per well in 96-well, collagen coated plates with no shaking. No overlay was used. Treatments were initiated 6 to 8 h after plating. Samples were run in triplicate and quenched with acetonitrile analogous to suspension hepatocyte incubations (1:1 volume, plates centrifuged to pellet protein). Negative controls, both cell-free assays and metabolically inactivated hepatocytes that had undergone 2 freeze-thaws, were run throughout the time course.

Bidirectional permeability (Caco-2) assay. To assess the impact of absorption on the IVIVE modeling, a subset of the chemicals for which *in vivo* PK data were available were tested in the bidirectional permeability assay (Wetmore *et al.*, 2012). These permeability assays were performed at Absorption Systems (Exton, Pennsylvania).

Chemical analysis by liquid chromatography with mass spectrometric detection. Samples from the metabolic stability assay (quenched 1:1 with acetonitrile) were thawed at room temperature, vortexed briefly, and centrifuged at 4500 × g for 5 min. Samples were then diluted with either 0.1% formic acid (FA) in hepatocyte media, for positive mode ionization, or 10mM ammonium acetate in hepatocyte media, for negative ionization mode. Samples from the 10 μM metabolic stability incubations were diluted 1:10, whereas the 1 μM incubations were diluted 1:4. Prior to analysis, samples were spiked with internal standard (Isoxaben [CAS 82558-50-7], Pirimicarb [CAS 23103-98-2] or Propoxur [CAS 114-26-1] for positive ion mode, 2,4-dichlorophenoxyacetic acid [CAS 94-75-7] or 2-methyl-4-chlorophenoxyacetic acid (MCPA) [CAS 94-74-6] for negative ion mode) and adjusted to contain approximately 25% total organic content using methanol. Samples were analyzed using either an API-3000 triple quadrupole mass spectrometer (Danaher, Washington, D.C.) with a PE-200 Perkin Elmer High Pressure Liquid Chromatography (HPLC) system (Perkin Elmer, Waltham, MA) or an Agilent 6460 triple quadrupole mass spectrometer (MS) with an Agilent 1290 Infinity ultra-HPLC (uHPLC) system (Agilent, Santa Clara, California). Calibration standards were prepared on the same day as sample analysis and in a matrix identical to the samples. Samples from the plasma protein binding assay (quenched 1:1:6, Plasma:PBS:Acetonitrile) were thawed at room temperature, vortexed briefly, and centrifuged at 12 000 × g for 4 min. All plasma samples were prepared as outlined earlier for the 1 μM metabolic stability assay samples (ie, 1:4 dilution). Detailed chromatographic separation protocols along with mass spectrometric (MS) information for all compounds analyzed by liquid chromatography (LC)/MS are provided in Supplementary Tables S2A–C.

Chemical analysis by selective ion-monitoring gas chromatography (GC) with mass spectrometric detection. Both metabolic stability assay samples and protein binding samples were obtained in the same dilutions described in the HPLC/MS methods earlier. All samples were thawed at room temperature, vortexed briefly, and centrifuged at 4500 × g for 5 min. Prior to liquid extraction, samples were spiked with a solution containing a known amount of internal standard and diluted 3:2 with a saturated NaCl solution for the metabolic stability assay samples and 2:3 for the protein binding samples. Samples underwent 1 hexane extraction (150 μl, nanograde quality), were vortexed briefly, allowed to equilibrate for 30 min, and centrifuged at 1300 × g for 2 min. The hexane layers were collected and transferred to silinated glass inserts prior to analysis using an Agilent 6890 gas chromatograph with a model 5973 MS (Agilent Technologies) in either electron impact mode or negative chemical ionization mode. Calibration standards were prepared on the same day as sample analysis and in a matrix identical to the samples. Sample data were collected in selective ion-monitoring (SIM) mode. Specific chromatographic separation details and instrumental parameters for each analyte are provided as Supplementary material (Supplementary Table S2D).

Chemical analysis by GC with electron capture detection. Both metabolic stability assay samples and protein binding samples were obtained using the same dilutions described in the HPLC/MS methods earlier. Samples were prepared following the same extraction method mentioned earlier. Sample data was collected with detector settings at 300°C with nitrogen makeup gas. Chromatographic separation details and analyte elution times are provided in the Supplementary materials section (Supplementary Table S2E).

Chemical analysis by HPLC with fluorescence detection (HPLC/FLD). Samples from both the metabolic stability assay and the protein binding assay were thawed at room temperature and briefly vortexed prior to centrifugation at 12 000 × g for 5 min. Samples were placed in silinated glass inserts and injected onto an Agilent 1100 HPLC with ultraviolet/fluorescent detectors (Agilent Technologies) without any additional sample work-up. Chromatographic separation details, fluorescence settings, and analyte elution times are described in the Supplementary materials section (Supplementary Table S2F–H).

Plasma protein binding data analysis. To calculate the fraction of unbound chemical in the plasma (F_u) from equilibrium dialysis data, the concentration of the test compound in the phosphate buffered saline (PBS) chamber was divided by the mean concentration in the matched plasma sample. Values derived for the 3 replicates were then averaged to determine a mean F_u. A minimum measurable F_u was set to 0.005. This value was estimated based on 2 SD over the minimum amount of binding detected in

a previous study (Waters *et al.*, 2008) and previous experience with the RED method (Rotroff *et al.*, 2010b; Wetmore *et al.*, 2012). If the concentration of the chemical in the free fraction was below, this value or below the analytical limits of detection, a default F_u of 0.005 was assumed.

To calculate F_u from the ultrafiltration data, the concentration of the test compound in the plasma ultrafiltrate was divided by the concentration in the precentrifugation sample for each replicate. The average mean percent unbound was calculated for the 3 replicates run. Mean percent unbound values were calculated in the same way for the NSB samples. Chemicals with NSB values exceeding 5% were excluded from further analyses. The plasma protein binding data are provided in Supplementary Table S3A.

Metabolic clearance data analysis. Hepatic metabolic clearance ($Cl_{in\ vitro}$) was determined following linear regression analysis of data measuring the loss of chemical over time (Rotroff *et al.*, 2010b; Wetmore *et al.*, 2012). Clearance was normalized to cell number [$\mu l/(min \times 10^6$ cells)]. The concentration data at each time point for each chemical and the linear regression results are provided as Supplementary Table S3B.

A NSB of a chemical that occurs may limit the amount of chemical available for clearance in an *in vitro* system (Hallifax *et al.*, 2010). Estimating clearance through loss of parent compound as done with the substrate depletion approach may lead to an underestimation of clearance for highly bound compounds. Although a nonspecifically bound chemical cannot be metabolized, it is still present in the incubation mixture and will be measured as part of the parent compound remaining. To account for the impact of this binding, $Cl_{in\ vitro}$ rates were converted to $Clu_{in\ vitro}$ using the following equation:

$$Clu_{in\ vitro} = \frac{Cl_{in\ vitro}}{fu_{hep}}$$

The fu_{hep} was calculated following (Kilford *et al.*, 2008) with log P/D values obtained from SciFinder (CAS). For those chemicals for which the fu_{hep} was calculated to be negative or > 1, a default value of 1 was used.

Estimation of C_{ss} using IVIVE and Monte Carlo *simulation*. The chemical steady-state blood concentrations (C_{ss}) were estimated as previously described (Wetmore *et al.*, 2012) with modification. The basic equation used to calculate static C_{ss} is based on constant uptake of a daily oral dose and factors in hepatic clearance and nonmetabolic renal clearance:

$$C_{ss} = \frac{ko}{\left(\frac{(Q_H \times F_{ub} \times Cl_{intH})}{(Q_H + F_{ub} \times Cl_{intH})}\right) + (GFR \times F_{ub})}$$

where ko = chemical exposure rate; mean Q_H = hepatic blood flow (90 l/h; Davies and Morris, 1993), F_{ub} = unbound fraction of parent compound in the blood; Cl_{intH} = hepatic intrinsic metabolic clearance; and GFR = glomerular filtration rate. The mean F_{ub} was calculated based on the experimentally measured F_u in plasma divided by the blood:plasma ratio (B:P). The right side of the denominator considers nonmetabolic renal clearance ($GFR \times F_{ub}$), with mean GFR (6.7 l/h) back-calculated based on the serum creatinine Cockcroft-Gault equation (Cockcroft and Gault, 1976). The Cl_{int} values were derived using the following equation, which scales $Clu_{in\ vitro}$ ($\mu l/(min \times$ million cells)) experimentally measured in hepatocytes to represent whole organ clearance with units of l/h:

$$Cl_{int} = Clu_{in\ vitro} \times HPGL \times V_l \times \frac{l}{10^6 \mu l} \times \frac{60\ min}{1\ h}$$

Where HPGL = hepatocytes per gram liver (110 million cells/g liver; (Barter *et al.*, 2007)) and V_l = liver volume (1596 g; Johnson *et al.*, 2005). The physiologic values employed in the Simcyp software are similar and in some cases identical to those utilized by other physiologically-based PK modelers; comparison of the outputs obtained from Simcyp to those obtained using values employed by other modelers resulted in similar outputs (data not shown).

Because the model for C_{ss} is linear in dose rate, C^1_{ss} was predicted for a dose rate of 1 mg/kg BW/day (ie, ko = 0.042 mg/kg/h). A correlated Monte Carlo approach was employed (Jamei *et al.*, 2009) using Simcyp (Simcyp V. 13; Certara, Sheffield, UK) to simulate variability across a population of 10 000 individuals equally comprised of both genders, 20–50 years of age. A coefficient of variation of 30% was used for intrinsic and renal clearance (Jamei *et al.*, 2009). The median, upper, and lower fifth percentiles for the C_{ss} were obtained as output. Additional background on this approach and related assessments of the C_{ss} outputs can be found in Wetmore *et al.*, 2012 and Wetmore, 2015.

Calculation and statistical presentation of OED data. As previously described, the *in vitro* AC_{50} (concentration at 50% of maximum activity) or lowest effective concentration (LEC) values were assumed to be functionally equivalent to the C_{ss} values in terms of biological activity (Rotroff *et al.*, 2010b; Wetmore *et al.*, 2012). Using reverse dosimetry (Tan *et al.*, 2007), the median, 5th, and 95th percentiles for the C_{ss} were used as conversion factors to generate OEDs according to the following formula:

$$OED\ \left(\frac{mg/kg}{d}\right) = \text{ToxCast}\ AC_{50}\ \text{or}\ LEC\ (\mu M) \frac{(1\ mg/kg)/day}{C^1_{ss}(\mu M)}$$

In the equation, the OED is linearly related to the *in vitro* AC_{50} or LEC and inversely related to C^1_{ss}. This equation is valid only for first-order metabolism that is expected at ambient exposure levels. An OED was generated for each chemical and each AC_{50} or LEC value across all of the *in vitro* assay endpoints.

Box and whisker plots were used to visualize the OEDs for each chemical. In each figure, the 95th percentile of the C_{ss} was used in the figures to provide a conservative estimate of the OEDs. The median OED for each chemical was displayed as a horizontal line and the ends of the boxes represent the 25th and 75th percentiles. The whiskers denote those values that fall either less than or greater than 1.5 times the interquartile range from the 25th or 75th percentiles, respectively (Tukey, 1977). In those instances where the minimum or maximum value for that chemical does not exceed the whisker, the whisker is set to that value. Any value beyond the range of the whiskers is designated as an outlier and is displayed as a black circle.

Evaluation of PK modeling. Published human *in vivo* PK data from which C_{ss} values could be derived were available for 16 of the 178 chemicals analyzed. These data characterized the observed total clearance from the body including hepatic metabolism and glomerular filtration as well as any other PK pathways present *in vivo*. To assess the predictivity of our IVIVE model, C_{ss} values were calculated using the measured *in vivo* values,

assuming a daily oral dose of 1 mg/kg/day. These values were then compared against the IVIVE-derived values obtained using the *in vitro* clearance rate derived using 1 μM chemical concentration. In addition, Caco-2 data was incorporated into the IVIVE to assess the impact of the assumption of 100% absorption on the prediction of C_{ss}. Further, for those chemicals that displayed no measurable clearance in the hepatocyte suspensions, plated hepatocytes were employed to measure clearance via substrate depletion over 48 h.

In vitro bioactivity data. To date, ToxCast bioactivity data includes measured bioactivity screening data across over 1000 compounds against a set of approximately 700 *in vitro* assay endpoints. Data from the December, 2014 release were downloaded from the ToxCast website (http://epa.gov/ncct/toxcast/data.html) [last accessed August 20, 2015]. Nine separate technologies were used, including receptor-binding and enzyme activity assays, cell-based protein and RNA expression assays, real time growth measured by electronic impedance, and fluorescent cellular imaging. Each chemical-assay combination was run in concentration response and an AC_{50} or LEC value was calculated, if applicable, depending on the range of the concentration response data. The data utilized include outputs from a new data processing pipeline http://epa.gov/ncct/toxcast/files/MySQL=20Database/Pipeline_Overview.pdf. In addition to revised AC_{50} outputs, data quality flags have been incorporated to alert users to experimental issues that may confound data interpretation. The chemical-assay hits of relevance for this study were reviewed for presence of a potential data quality issue, indicated by 1 of 17 flags that encompass issues across all of the ToxCast assay platforms (for more information, visit http://epa.gov/ncct/toxcast/data.html). Given that many of the flags are platform-specific and this assessment was comprehensive, spanning all chemical-assay hits across all of the technologies but with a focus on the most potent AC_{50} for AER derivation, any of these hits tagged with any flag was removed from the assessment. Although not the most conservative approach, this method using the higher confidence *in vitro* bioactivity results was selected for an illustrative example. The original list of 8963 chemical-assay hits across the 178 chemicals was thus filtered down to a list of 4582 hits across 163 of the chemicals.

Several peer reviewed publications utilizing the bioassay data from Phase I (Houck *et al.*, 2009; Huang *et al.*, 2011; Judson *et al.*, 2010; Kleinstreuer *et al.*, 2014; Knight *et al.*, 2009; Knudsen *et al.*, 2011; Martin *et al.*, 2010; Rotroff *et al.*, 2010a, 2013) and 2 from Phase II (Kleinstreuer *et al.*, 2014; Sipes *et al.*, 2013) are available and provide additional information. A detailed description of the chemicals screened, assays used and details related to the new pipeline outputs can be found at the USEPA download site (http://epa.gov/ncct/toxcast/data.html).

Exposure prediction methods. A probabilistic exposure modeling approach was employed, as detailed in (Wambaugh *et al.*, 2014). Briefly, subject-specific NHANES urinary analyte data were collected and analyzed in a reverse PK approach that used a parent-to-analyte mapping to infer parent compound exposure for 106 chemicals. Because there were multiple combinations of parent chemical exposures that were consistent with the analyte data, a range of possible combinations of inferred parent chemical exposures was analyzed. Chemicals were assigned indicator variables (with value 1 or 0 corresponding to yes or no) indicating evidence for use of that chemical within broad use categories (eg, consumer use, pesticide active) based on listings in U.S. EPA's ACToR (Aggregated Computational Toxicology Resource) database (Dionisio *et al.*, 2015). Chemicals were further characterized using physico-chemical properties and national production volume data. These simple chemical descriptors were chosen because they were available for thousands of chemicals.

To identify those factors that most correlated with the range of inferred chemical exposures, Wambaugh *et al.* (2014) assumed a linear model in which the logarithm of inferred parent exposure depended on an average value and, potentially, some factors among production volume, chemical use indicator variables, and physico-chemical properties. Each of the factors in the linear model were scaled and centered and multiplied by a weight that indicated the relative importance to the model. The selection of the most predictive factors was performed using the method of best subsets to estimate regression weights best subset selection was performed using complete enumeration of factor combinations (Morgan and Tatar, 1972). This process was repeated across the range of possible chemical exposure scenarios to identify the minimum number of factors required to build a parsimonious model, using the average Akaike information criterion (AIC) (Akaike, 1974) across the scenarios. A 5-factor model was suggested by AIC. The frequency of occurrence of the factors among the best subset size was used to determine the optimal model.

Using the factors identified by the best subsets analysis a second Bayesian regression was performed to jointly infer the regression coefficients, stoichiometric relationships among metabolites, and parent exposures from the NHANES urinary data. This joint Bayesian analysis was performed separately for the entire NHANES samples (roughly 2000 individuals per chemical) and subsets of that sample corresponding to 9 demographic groups and life stages, including: children 6–11 years of age, children 12–19 years of age, adults 20–65 years of age, females adults (6–85), males (6–85), adults older than 65 years, females of child-bearing age (16–49), and adults older than 65 years of age (65–85). Also assessed were adults (mixed gender, age range) with a body mass index (BMI) < 30 and a BMI > 30. A calibrated model based on the same 5 factors was found to be predictive across all groups.

The Wambaugh *et al.* (2014) calibrated model explained roughly 50% of the chemical-to-chemical variance within the biomonitoring data. The remaining unexplained variance served as an empirical estimate of the uncertainty in the predictions, due to assumptions of the modeling, measurement limitations of the data, quality issues in the chemical descriptors, and any other factor not taken into account by the modeling analysis of the 106 chemicals that could be inferred from NHANES urine analytes. Both the calibrated model and empirical estimate of the uncertainty were extrapolated to predict exposure for chemicals without biomonitoring data. The Bayesian analysis was used to predict geometric mean population exposures with 95% credible intervals around the mean estimates. The model weights and chemical-specific predictions and descriptors are given in Wambaugh *et al.* (2014).

RESULTS

Evaluation of PK Modeling

Of the 16 chemicals for which C_{ss} values were derived from published human *in vivo* PK data, 11 were within 10-fold of the IVIVE-derived C_{ss} predictions (Table 1). When the IVIVE was

TABLE 1. Comparison of IVIVE C_{ss} Predictions with Published *In Vivo*–Derived Values

Chemical	C_{ss} Values (μM)				Fold Difference			
	In Vivo	IVIVE Suspended	IVIVE Caco-2 Suspended	IVIVE Caco-2 Plated	HT	Refined	Key to Prediction Improvement	References for *In Vivo* Calculations
Acetaminophen	1.1[a]	0.52	0.57	—	0.5	0.5	Within 2-fold	(Critchley *et al.*, 2005; Gelotte *et al.*, 2007; Rostami-Hodjegan *et al.*, 2002)
2-chloro-2′deoxyadenosine	0.28	1.36	0.58	0.31	4.9	1.1	Within 5-fold	(Lindemalm *et al.*, 2005)
5,5′-diphenylhydantoin	4.92	1.59	1.59	—	0.3	0.4	Within 4-fold	(Brien *et al.*, 1975)
6-propyl-2-thiouracil	1.1[a]	1.58	1.80	—	1.3	1.5	Within 2-fold	(Giles *et al.*, 1981; Kabanda *et al.*, 1996)
Candoxatril	0.023	0.18	0.14	—	7.8	6.1	Within 6-fold	(Kaye *et al.*, 1997)
Chlorpyrifos	0.022	0.24	0.27	—	10.9	12.3	Unknown	(Nolan, 1984, 371)
Coumarin	0.01–0.02	13.63	15.40	1.73	681–1363	87–173	Plated hepatocytes Other; unknown	(Lamiable *et al.*, 1993; Mielke *et al.*, 2011)
Diphenhydramine HCl	0.11–0.16	3.18	3.57	0.66	20–29	4–6	Plated hepatocytes	(Albert *et al.*, 1975; Blyden *et al.*, 1986; Luna *et al.*, 1989; Toothaker *et al.*, 2000)
Flutamide	0.004–0.005	0.57	0.64	—	142	160	Inclusion of intestinal metabolism	(Anjum *et al.*, 1999; Doser *et al.*, 1997; Radwanski *et al.*, 1989)
Haloperidol	0.126	0.07	0.08	—	1.8	1.6	Within 2-fold	(Yasui-Furukori *et al.*, 2002)
Lovastatin	0.004–0.009	0.16	0.18	—	18–40	20–45	Unknown	(Bramer *et al.*, 1999; Kothare *et al.*, 2007; Mignini *et al.*, 2008)
PK 11195	0.14	0.58	0.66	—	4.1	4.7	Within 5-fold	(Ferry *et al.*, 1989)
Sulfasalazine	0.2–1.8	11.6	2.5	—	7–48	1–10	Caco-2	(Adkison *et al.*, 2010; Gu *et al.*, 2011; Ma *et al.*, 2009)
Triamcinolone	0.05–0.29	0.22	0.11	—	0.8–4.4	0.4–2.2	Within 5-fold	(Argenti *et al.*, 2000; Derendorf *et al.*, 1995; Hochhaus *et al.*, 1990)
Volinanserin	0.04	0.03	0.03	—	3.8	4.3	Within 4-fold	(Andree *et al.*, 1998)
Zamifenacin	2.86	0.57	0.64	—	0.2	0.2	Within 5-fold	(Beaumont *et al.*, 1996)

[a]Values from 2 studies were 1.05 and 1.12; for purposes of this work, 1.1 μM was used as comparator.

refined through the incorporation of Caco-2 data (to replace our assumption of 100% absorption with experimental data) and of revised clearance data using plated hepatocytes, predictions for 12 of the 16 compounds came within 6-fold of the IVIVE values. The 4 chemicals that performed poorly were all overpredicted: chlorpyrifos (12-fold), coumarin (87- to 173-fold) flutamide ((160-fold), and lovastatin (20- to 45-fold). Although better C_{ss} agreement is preferred, an overprediction provides a conservative or protective value. Thirteen of the 16 chemicals were overpredicted using the HT-IVIVE. The 3 that were underpredicted, however, were within 3- to 5-fold of the *in vivo* values. Incorporation of Caco-2 and revised clearance data increased the model predictivity for 2 and 3 of the 16 chemicals, respectively.

Distribution Analysis of AC_{50} and C_{ss} Values

Distribution analysis of the minimum AC_{50} values derived for each chemical across all assay technologies revealed that the minimum value was 7.4E-05 μM for diethylstilbesterol. The median was 1.6 μM, with the lower 5th, 10th, and 25th percentiles at 0.004, 0.012, and 0.259 μM, respectively (Fig. 1A). The highest minimum AC_{50} value was 91.4 μM for 1,3-diisopropylbenzene. Assessment of the C_{ss} values derived via IVIVE modeling, assuming an oral administration of 1 mg/kg/day across the 178 Phase II chemicals, revealed a median C_{ss} value of 0.94 μM, with approximately 80% of the chemicals possessing values < 10 μM (Fig. 1B). Moreover, the upper 95th percentile was 230 μM, with approximately 7% of the chemicals possessing a $C_{ss} > 200$ μM.

Influence of C_{ss} on In Vitro Bioactivities

To demonstrate the impact of incorporating chemical steady-state behavior on *in vitro* bioactivity values, Table 2 displays the range of OEDs that result across 14 chemicals (with hits listed across 18 assay endpoints) that exhibited bioactivity at an AC_{50} value of 1 μM. The minimum and maximum OEDs ranged from 0.002 (dinoseb) to 51 mg/kg/day (butylparaben), spanning over 4 orders of magnitude (25 000-fold). OEDs for 9 of the 18 chemicals were within 5-fold of each other, with values ranging from 0.31 to 1.47 mg/kg/day.

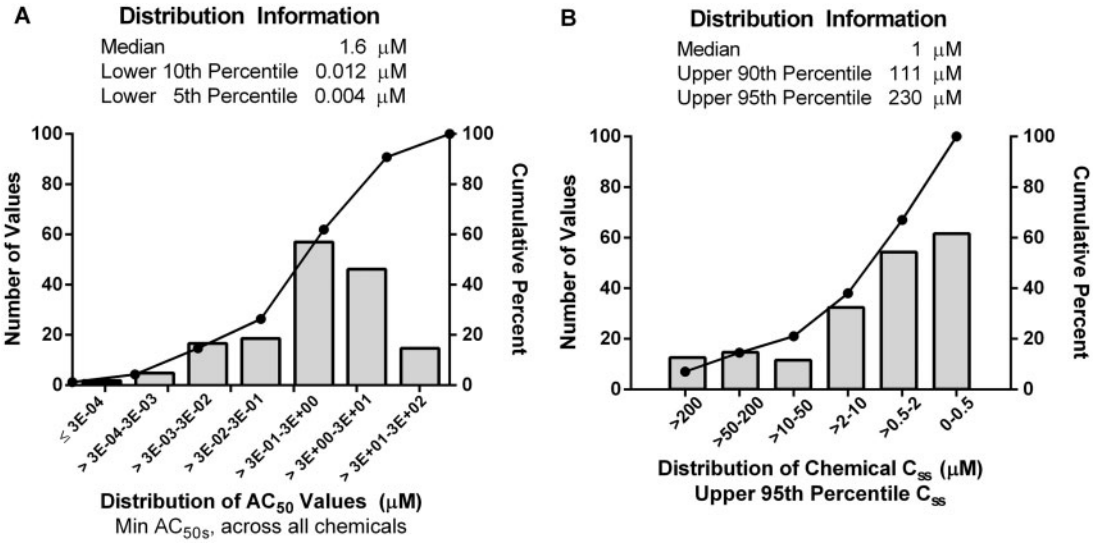

FIG. 1. Distribution and summary statistics of activity concentration (AC_{50}) and C_{ss} values. A, The minimum AC_{50} values derived across all technologies for each chemical underwent distribution analysis and were binned across 7 concentration ranges to display the number of values (bar graph) and cumulative frequency (line graph) across the relevant range, with the summary statistics provided. B, The 95th percentile C_{ss} values (μM) was predicted using the hepatic chemical clearance rate measured at 1μM across a population of 10 000 individuals (using Monte Carlo simulation, assuming a unit dose rate of 1 mg/kg/day; see Materials and Methods) were binned and displayed in a manner similar to A. Values are provided from highest to lowest as a higher predicted C_{ss} may indicate a higher chemical exposure. Summary statistics are also provided.

TABLE 2. Oral Equivalent Dose Ranges for Chemicals with Identical *In Vitro* Potencies but Varied Steady-State Behavior

Chemical	C_{ss}[a] (μM)	Assay Endpoint	AC_{50} (μM)	OED[b] (mg/kg/day)
Dinoseb	485.94	Agonist for p53 signaling pathway in HCT-116 cells	1	0.002
Gentian violet	10.01	Decreased expression of tissue matrix metalloprotease inhibitor-2 in human keratinocytes	1	0.095
Gentian violet	10.01	Binding to muscarinic acetylcholine receptor M2	1	0.096
Gentian violet	10.01	Decreased expression of urokinase receptor in human endothelial cells	1	0.098
Didecyl dimethyl ammonium chloride	3.37	Decreased expression of collagen type III in human primary fibroblasts	1	0.306
Dieldrin	2.32	Activation of estrogen receptor response element in transfected HepG2 cells	1	0.431
2-Chloro-2′-deoxyadenosine	2.07	Decreased expression of membrane protein CD40 in human endothelial cells	1	0.464
9-Phenanthrol	2.14	Decreased proliferation of human primary fibroblasts	1	0.481
Ethion	1.40	Activation of the phenobarbital-responsive enhancer module in transfected HepG2 cells	1	0.711
Pentachlorophenol	0.87	Inhibition of the peroxisome proliferator-activated receptor gamma signaling pathway in HEK293 cells	1	1.143
o,p-DDT	0.80	Activation of estrogen receptor response element in transfected HepG2 cells	1	1.232
Zamifenacin	0.69	Binding to guinea pig dopamine transporter	1	1.457
Zamifenacin	0.69	Binding to human 5-hydroxytryptamine-7 (5HT7) receptor	1	1.471
Benz[a]anthracene	0.47	Increased expression of matrix metalloprotease-1 in human primary bronchial epithelial cells	1	2.053
Diethylstilbesterol (DES)	0.46	Inhibition of rat CYP2C13 enzymatic activity	1	2.151
N-Phenyl-1,4-benzenediamine	0.33	Decreased expression of tissue factor in human endothelial cells	1	2.927
Butylparaben	0.02	Activation of estrogen receptor alpha signaling pathway in transfected HepG2 cells	1	51.140

[a]C_{ss}, Concentration at steady state.
[b]OED, oral equivalent dose.

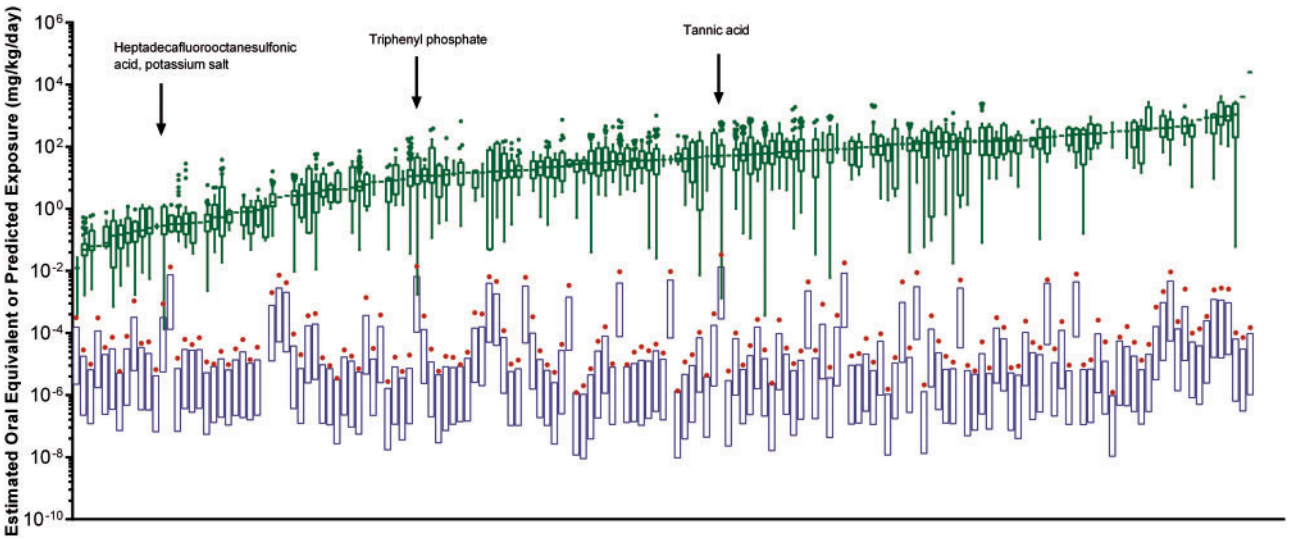

FIG. 2. Comparison of human oral equivalent doses (OEDs) and exposure predictions for 163 ToxCast Phase II chemicals. Distributions of the OEDs across approximately 700 *in vitro* assays for each chemical are depicted as box-and-whisker plots, presented with exposure predictions derived from (Wambaugh *et al.*, 2014). Data are ordered from lowest to highest median OEDs. A full list of chemicals and supporting data are provided in Supplementary Table S4. Predicted exposures are represented by floating bars, with the lower bar value representing the geometric mean and the upper bar the upper 95% confidence limit around the mean. The red filled circle denotes the upper 95% confidence limit derived for the most highly exposed (MHE) population for that chemical. Arrows indicate chemicals with AERs < 1.

Assessment of Exposure Predictions

The HT exposure method makes chemical-specific predictions for the geometric mean for U.S. populations. Uncertainty in the estimates is characterized by a 95% confidence. The upper 95% confidence limit of the geometric mean ranged from 9.26E-07 mg/kg/day (methyl eugenol) to a maximum of 8.46E-03 mg/kg/day (di(2-ethylhexyl)adipate). The range of the 95% confidence limits were on average 4 orders of magnitude. Comparison of the predictions for the total population against the most highly exposed (MHE) population for each chemical revealed that the MHE values were on average 2- to 3-fold higher (Supplementary Table S4). However, for the HT exposure model that was used, there were no statistically significant differences in the mean prediction by the model for the various populations. For instance, of the 163 chemicals assessed, the 2 BMI groups (BMI > 30 and BMI < 30) emerged as being the predominant MHE population for 32 and 31 chemicals, respectively (Supplementary Table S4). This finding is likely artifactual due to the relatively sensitive nature of the 95th percentile to the relative sizes of the sample populations analyzed. The third most prevalent MHE population was the 12- to 19-year-old group, for 26 chemicals.

Assessment of Dosimetry-Adjusted ToxCast *Assay Activity With HT Exposure Predictions*

Figure 2 displays the range of OEDs derived for each chemical across all relevant assays in a box and whisker format, superimposed with floating bars that provide HT exposure predictions (Wambaugh *et al.*, 2013, 2014). In Figure 2, the floating bars represent the predictions across the total population, with the median assigned the lower bound value and upper 95% of the credible interval around the median assigned the upper-bound value. The red circle represents the upper 95% confidence interval for the MHE population.

Of the 178 chemicals for which hepatic clearance and plasma protein binding were successfully measured, 163 possessed at least 1 ToxCast assay in which bioactivity was observed/measurable (ie, an AC_{50} or LEC was estimated). HT exposure predictions were available for all 163 chemicals. AERs were calculated for each chemical by dividing the minimum OED (ie, the most potent assay for that chemical) by the upper bound of the 95% confidence interval of the geometric mean for the exposure predictions. When AERs were calculated using the upper-bound exposure predictions for the total population, 3, 6, and 13 chemicals possessed AERs < 1, 10, and 100, respectively. When AERs were calculated using the upper-bound predictions for the MHE populations, 5, 9, and 19 chemicals possessed AERs < 1, 10, and 100, respectively (Supplementary Table S4). Distribution of the AERs across the Phase II chemicals assessed in this study revealed median values of 2.04E+04 and 9.58E+03 for the total and MHE populations, respectively (Fig. 3).

Closer inspection of the twenty chemicals with the lowest AERs revealed that organofluorines and insecticides previously withdrawn from the market comprised 5 of the 12 chemicals (Table 3). Tannic acid, a plant polyphenol with food and drug uses yielded the lowest AER (MHE AER 0.017 mg/kg/day). This was derived based on an OED of 5.83E-04 mg/kg/d for a cell-free assay measuring glycogen synthase kinase 3 beta (GSK3b) activation, an enzyme involved in energy metabolism and neuronal development (Plyte *et al.*, 1992). Of the 12 chemicals with AERs < 1, only 2—naphthalene (6 hits) and organofluorine heptadecafluorooctanesulfonic acid, potassium salt (2 hits)—had bioactivities measured in more than 1 assay. A complete listing of chemicals, associated uses and specific information for all assays that yielded an AER < 10 is provided in Supplementary Table S4.

Assessment of the OED Findings

The potency of a chemical's OED could be due to either a low ToxCast assay AC_{50} value (ie, potent activity), a high C_{ss} value resulting from the IVIVE, or a combination of the 2. A subset of chemicals possessing low OEDs was more closely examined to assess the relative contribution of these 2 factors on the final values across this chemical space. Of the 11 chemicals that possessed OEDs < 1 μg/kg/day, 3 were perfluorinated compounds, 3 were insecticides which had been withdrawn from the market, 2 were pharmaceutical compounds, and 1 a plant polyphenol (Table 3). All but 2 of the chemical-assay hits possessed an

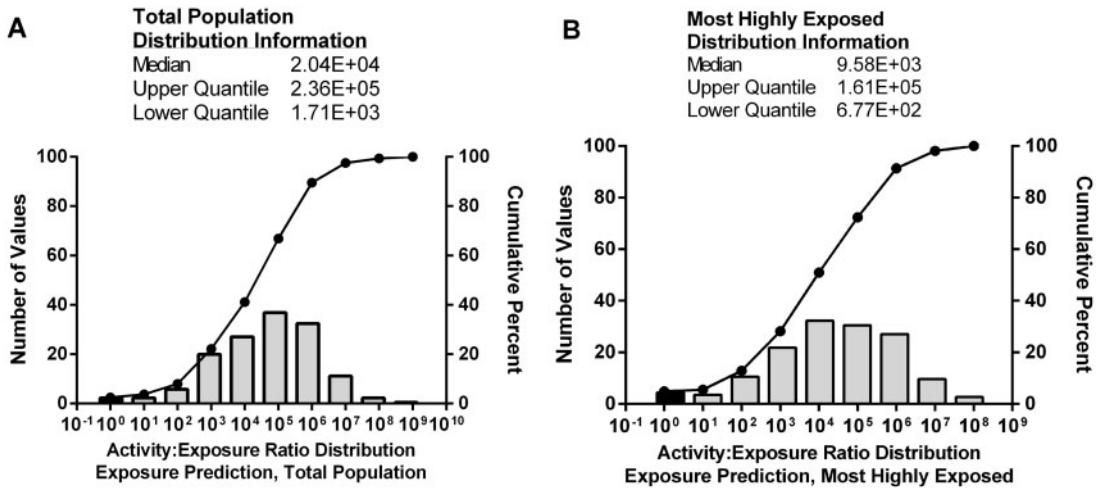

FIG. 3. AER distribution across the ToxCast Phase II chemicals assessed. Histograms and cumulative percent data (line graph) are displayed to capture the AER distribution across the chemicals analyzed for the total population (A) and the MHE population (B). AERs are calculated by dividing the minimum chemical OED by the upper 95% confidence limit around the mean exposure prediction (see Materials and Methods). The bar representing chemicals with AERs < 1 are colored black. Summary statistics are also provided.

$AC_{50} < 0.5\,\mu M$. Six of the eleven chemicals possessed a $C_{ss} > 200\,\mu M$—a criterion representative for the upper 10th percent of all chemicals. Three of the 6 chemicals with high C_{ss} values were organofluorines, most of which had former uses as flame retardants.

DISCUSSION

To assess the utility of *in vitro* HTS data to predict chemical hazard to human health, the USEPA ToxCast program has evaluated libraries of chemicals in multiple phases. Phase I assessments screened and analyzed data-rich compounds, in particular food-use pesticides, for which measured physicochemical properties, *in vivo* hazard data, and exposure estimates were available. Knowledge of animal study-based apical responses enabled the assessment of the HTS data for their ability to identify biological pathway alterations (Houck *et al.*, 2009; Judson *et al.*, 2011; Knudsen *et al.*, 2011; Rotroff *et al.*, 2010a) and prediction of *in vivo* effects (Kleinstreuer *et al.*, 2011; Martin *et al.*, 2011; Sipes *et al.*, 2011; Thomas *et al.*, 2012; Wetmore *et al.*, 2013). Efforts to incorporate chemical dosimetry with HTS data provided an *in vivo* context to the *in vitro* data, allowing an estimation of external dose required to achieve internal bioactivity-inducing concentrations (Rotroff *et al.*, 2010b; Wetmore *et al.*, 2013, 2012). These studies have both indicated the potential of ToxCast data as a risk-based prioritization tool (Judson *et al.*, 2011; Kavlock *et al.*, 2009; Krewski *et al.*, 2014) as well as identifying its limitations (Cox *et al.*, 2014; Thomas *et al.*, 2012; Wetmore *et al.*, 2013). The data and subsequent analyses have provided useful guidance as successive phases have been undertaken.

Chemicals in the Phase II library were selected to expand the chemical space addressed in Phase I and include banned and withdrawn pharmaceutical and industrial compounds along with compounds currently in commerce (Judson *et al.*, 2009). Inclusion of pharmaceuticals for which therapeutic activities are already established—and banned chemicals with well recognized *in vivo* apical responses—allows an informed assessment of the bioactivities and potencies observed within the ToxCast dataset. However, only a limited number of these chemicals possess exposure information. In previous work combining HTS data with exposure (Wetmore *et al.*, 2012), review of USEPA reregistration eligibility documents and data collected by the CDC NHANES effort provided exposure data for over 80% of the ToxCast Phase I chemicals. When applied to the Phase II chemicals assessed in the current study, data were available for many fewer compounds, only 7%.

We addressed this in this study by employing a probabilistic modeling approach to approximate exposures in a HT manner (Wambaugh *et al.*, 2014). Even with the 4 order of magnitude span of the 95% credible interval around the geometric mean exposure predictions (Fig. 2), the ability to compare the upper-bound predictions against dosimetry-adjusted bioactivities provides a needed, risk-based strategy that can be applied in prioritization strategies. Further, as refined exposure modeling strategies emerge, their values could be readily incorporated with *in vitro* data to either refine lower tier assessments or lay the groundwork for strategies to be applied in higher tiers that require more data.

Review of the Phase II chemical AER findings provides insight into future priorities in exposure modeling efforts. The frequency of AERs < 1 derived in this assessment were significantly less than if predictions from an earlier version of this modeling approach (Wambaugh *et al.*, 2013) were employed (data not shown). This decrease is due in large part to the ability of the second model to explain 50% of the variability after assessment across multiple chemical product and use descriptors as opposed to 20% for a model based on far-field fate and transport models (Wambaugh *et al.*, 2013). Recent—and future—efforts that increase availability of chemical use and product formulation information should help significantly in refining near-field modeling tools and reducing uncertainty around the estimates to provide more accurate exposure predictions (Dionisio *et al.*, 2015; Goldsmith *et al.*, 2014). It should be noted that an AER cutoff of 1 is used primarily for illustrative purposes. Given that the upper-bound exposure predictions reflect the upper 95th percent confidence limit around the geometric mean, these values do not reflect an approximation of exposures to a sensitive population. Given this, a higher AER cutoff (eg, 100) may be more appropriate to consider in such strategies.

Phase II AER assessment also outlined important considerations related to HTS data interpretation. For instance, for all but 1 of the 7 chemicals flagged using the 2014 exposure model, only 1

TABLE 3. Use and Assay Information for Chemicals with the 20 Lowest Activity:Exposure Ratios

Chemical	Description/Use	No. Assay Hits Where MHE[a] AER[b] < 100	AC_{50} (μM)[c]	Oral Equivalent[c] (mg/kg/day)	Exposure Total (MHE) (mg/kg/day)	AER (MHE AER)
Tannic acid	Plant polyphenol; food, drug uses; mordant during dyeing process	5	0.0002	5.83E-04	1.35E-02 (3.36E-02)	0.043 (0.02)
Triphenyl phosphate	Plasticizer; fire retardant	3	0.0006	7.66E-04	6.57E-03 (1.41E-02)	0.117 (0.054)
Heptadecafluorooctanesulfonic acid potassium salt	Organofluorine	12	0.013	5.99E-05	3.21E-04 (8.72E-04)	0.187 (0.069)
Mirex	Banned organochlorine insecticide	3	0.01144	1.61E-04	1.55E-04 (3.13E-04)	1.040 (0.516)
Ammonium perfluorooctanoate	Organofluorine	9	0.20182	7.48E-04	3.24E-04 (1.09E-03)	2.310 (0.684)
Tributyl phosphate	Solvent; plasticizer	3	1.28	2.04E-02	4.03E-03 (6.60E-03)	5.05 (3.09)
Potassium perfluorohexanesulfonate	Organofluorine	2	0.0825	3.09E-04	3.09E-05 (7.27E-05)	10.02 (4.26)
Dioctyl phthalate	plasticizer	6	4.88	7.62E-02	7.49E-03 (1.34E-02)	10.18 (5.68)
DES	Nonsteroidal estrogen	6	0.000074	1.61E-04	1.49E-05 (2.84E-05)	10.82 (5.68)
Diphenhydramine hydrochloride	Antihistamine drug	2	0.0238	4.91E-03	1.95E-04 (4.27E-04)	25.21 (11.51)
Dinoseb	Herbicide	6	0.35	7.20E-04	1.76E-05 (2.87E-05)	40.81 (25.12)
Oxytetracycline hydrochloride	antibiotic	1	0.004	3.17E-03	7.11E-05 (1.06E-04)	44.64 (29.92)
1,2-Benzisothiazolin-3-one	Microbicide; fungicide	4	0.424	5.89E-02	7.78E-04 (2.00E-03)	75.69 (29.48)
Didecyl dimethyl ammonium chloride	Biocide; disinfectant	2	0.0139	4.13E-03	3.81E-05 (9.34E-05)	108.34 (44.18)
Perfluorononanoic acid	Organofluorine	1	0.601	2.39E-03	2.20E-05 (5.17E-05)	108.39 (46.18)
Perfluorodecanoic acid	Organofluorine	1	0.877	3.87E-03	3.46E-05 (4.66 E-05)	111.80 (82.95)
4-(2-methylbutan-yl)phenol	phenol	1	0.634	2.31E-01	1.85E-03 (4.58E-03)	125.23 (50.43)
Benzophenone	UV blocker; packaging	1	0.306	4.85E-01	2.81E-03 (5.14E-03)	172.37 (94.21)
Endrin	Organochlorine	[d]	0.272	1.14E-03	6.55E-06 (9.97E-06)	174.43 (114.51)
Gentian violet	Dye; topical antifungal drug	1	0.01	9.99E-04	5.27E-06 (1.17E-05)	189.56 (85.05)

[a]MHE, most highly exposed.
[b]AER, activity-to-exposure ratio.
[c]Values listed are associated with the most potent assay for each chemical. Values associated with other chemical-assay hits (where relevant) are listed in Supplementary Table S4.
[d]All AERs returned for this chemical exceeded 100.

or 2 assay hits per chemical resulted in an AER < 1. The ToxCast assays were originally selected from those that were commercially available and in use by the pharmaceutical industry and, as such, the bioactivities interrogated in ToxCast focus primarily on therapeutic or receptor-mediated events. Consequently, closer examination of specific hits is warranted to differentiate biologic perturbations from measures of adversity. Importantly, HTS hits for certain pharmaceuticals in this list were consistent with their therapeutic target (Supplementary Table S4).

Comparison of the IVIVE-based predictions against *in vivo* data revealed that this simplified IVIVE strategy did reasonably well in predicting *in vivo* PK behavior: 12 of the 16 chemicals assessed coming within 10-fold of the predictions (Table 1). For the 4 that exceeded 10-fold, the C_{ss} values were all overpredicted. Three chemicals were underpredicted, but these were within 2- to 5-fold of the *in vivo* values. Flutamide, an antiandrogen drug used in the treatment of prostate cancer, was overpredicted by over 100-fold. Flutamide undergoes extensive first-pass metabolism, hydrolyzed primarily by carboxylesterase 2 and arylacetamide deacetylase, 2 major serine esterases expressed in both the liver and the intestine (Imai and Ohura, 2010; Kobayashi *et al.*, 2012). The C_{ss} overprediction is likely due to the lack of consideration of extrahepatic metabolism in the IVIVE model. In addition, the chemicals for which the IVIVE model yielded the poorest agreement, including flutamide, all possessed relatively low *in vivo* C_{ss} values of < 0.03 μM

TABLE 4. Corresponding Dosimetry and Assay Information for Chemicals with OEDs < 1 μg/kg/day

Chemical	C_{ss} (μM)	Assay Endpoint	AC_{50} (μM)	Oral Equivalent (mg/kg/day)	C_{ss} > 200 (μM)	AC_{50} < 0.5 (μM)
Heptadecafluorooctanesulfonic acid potassium salt	217.01	Inhibition of human CYP2C9 enzymatic activity	1.30E-02	5.99E-05	Yes	Yes
Mirex	70.82	Increased expression of prostaglandin E2 in human peripheral blood mononuclear cells	1.14E-02	1.61E-04	—	Yes
Diethylstilbestrol	0.46	Binding to human estrogen receptor	7.43E-05	1.61E-04	—	Yes
Diethylstilbestrol	0.46	Activation of estrogen receptor response element in transfected HepG2 cells	1.01E-04	2.19E-04	—	Yes
Diethylstilbestrol	0.46	Activation of estrogen receptor signaling pathway in transfected HEK293 cells	1.27E-04	2.76E-04	—	Yes
Potassium perfluorohexanesulfonate	266.56	Inhibition of human CYP2C9 enzymatic activity	8.25E-02	3.09E-04	Yes	Yes
Potassium perfluorohexanesulfonate	266.56	Inhibition of human CYP4F12 enzymatic activity	8.60E-02	3.23E-04	Yes	Yes
Diethylstilbestrol	0.46	Activation of estrogen receptor alpha signaling pathway in transfected HepG2 cells	1.80E-04	3.92E-04	—	Yes
Tannic acid	0.34	Inhibition of human GSK3b enzymatic activity	2.00E-04	5.83E-04	—	Yes
Dinoseb	485.94	Decreased mitochondrial membrane potential in HepG2 cells	3.50E-01	7.20E-04	Yes	Yes
Pentadecafluorooctanoic acid ammonium salt	269.96	Inhibition of human CYP2C9 enzymatic activity	2.02E-01	7.48E-04	Yes	Yes
Triphenyl phosphate	0.79	Binding to human peroxisome proliferator-activated receptor-gamma	6.09E-04	7.66E-04	—	Yes
Diethylstilbestrol	0.46	Activation of estrogen receptor signaling pathway in transfected HEK293 cells	4.02E-04	8.73E-04	—	Yes
Gentian violet	10.01	Decreased expression of interleukin-8 in human peripheral blood mononuclear cells	1.00E-02	9.99E-04	—	Yes
Gentian violet	10.01	Decreased expression of E-selectin adhesion protein in human endothelial cells	1.00E-02	9.99E-04	—	Yes
Gentian violet	10.01	Decrease expression of interleukin 1 alpha in human peripheral blood mononuclear cells	1.00E-02	9.99E-04	—	Yes
Endrin	238.20	Activation of estrogen receptor response element in transfected HepG2 cells	2.72E-01	1.14E-03	Yes	Yes
Dinoseb	485.94	Decreased expression of transforming growth factor-beta in human primary bronchial epithelial cells	6.28E-01	1.29E-03	Yes	—
2-Methyl-4,6-dinitrophenol	589.15	Decrease mitochondrial membrane potential in HepG2 cells	8.74E-01	1.48E-03	Yes	—

compared to the other chemicals. This suggests that the conservative assumptions employed in the IVIVE model limit our ability to adequately predict blood C_{ss} values for those chemicals that are highly cleared *in vivo*. Indeed, coumarin, flutamide, and lovastatin all possess *in vivo* blood C_{ss} values of 0.01 μM or lower, down to 0.004 μM for flutamide. Of these 3 chemicals, the lowest predicted value was obtained for lovastatin, at 0.18 μM.

Additional work was performed to ascertain the impact of certain model assumptions and experimental design considerations on the predictive performance of the IVIVE. First, intestinal permeability data were obtained using the Caco-2 model and incorporated into the IVIVE to assess the impact of our assumption of 100% intestinal absorption. Caco-2 data improved the predictive performance of 3 of the 16 chemicals assessed, although 2 of these 3 chemicals were already predicted to be within 5-fold of the *in vivo* values using the conservative assumption. When these data are combined with equivalent data for Phase I chemicals (Wetmore *et al.*, 2012), the assumption of 100% intestinal absorption appears to be adequate for over 85% of the chemicals, because incorporation of Caco-2 data significantly improved the predictions for only 4 of the 29 chemicals assessed.

Use of pooled donor hepatocyte suspensions to measure hepatic clearance as performed here is considered to be the method of choice, as this system more accurately captures *in vivo* clearance than other available *in vitro* systems (Hallifax *et al.*, 2010; Li *et al.*, 1999; Pelkonen *et al.*, 2013) while minimizing the impact of donor variability. However, hepatocyte suspensions are not suitable for quantitating clearance of low turnover compounds with $Cl_{in\ vitro} < 2$ μl/(min × 10^6 cells), likely due to depletion of cofactor reserves over the 240 min time course (Houston *et al.*, 2012). Three of the 16 chemicals for which no measurable clearance was detected were also assessed using plated hepatocytes over a 48-h time course. Clearance was detected in this more sensitive system and improved the IVIVE predictions, particularly for coumarin and diphenhydramine HCl (Table 1). However, use of plated systems requires consideration of additional factors. First, culture conditions are known to alter activity of cytochrome P450 enzymes, so attention to plating methods and characterization of enzyme activity should be monitored. Second, donor pools cannot be successfully used in these plated systems currently (Smith *et al.*, 2012), so assessments across multiple donors need to be conducted to accurately determine variability in $Cl_{in\ vitro}$.

Inclusion of a range of pharmaceuticals and other chemical families (eg, organoflurorines, persistent organic pollutants, etc.) in the Phase II list provided an opportunity to assess the contribution of potent bioactivities or chemical pharmacokinetics to relatively low OEDs relative with these compounds. Eleven chemicals (approximately 7% of total assessed) were identified as having an OED < 1 μg/kg/day, across 19 assay endpoints (Table 4). The main driver for a potent OED was AC_{50} potency rather than a high C_{ss}. Interestingly, only 2 of these 11 chemicals were drugs: the synthetic nonsteroidal estrogen diethylstilbesterol and Gentian violet, an antiseptic dye with antibacterial and antifungal properties. Regardless, most of the assay hits were related to anti-inflammatory and other drug target activity (eg, IL-8, IL1-α downregulation; CYP2C9, CYP4F12). The work described here uses presence and potency of a ToxCast hit—without regard for chemical mode of action or adverse outcome—as a conservative strategy that is appropriate in prioritization efforts. However, the context and nature of these activities will need to be more carefully considered as related efforts—particularly those that go beyond prioritization—move forward.

The ToxCast and ExpoCast programs were designed to address the chemical safety needs of the USEPA through development and implementation of HT toxicity testing and exposure modeling strategies. By incorporating recent outputs of these 2 programs, this study provides an up to date assessment of the status of these efforts. It has also identified areas that warrant further attention. Refinement of HT hazard estimates to identify relevant modes of action and downstream adverse effects would arguably provide a more appropriate basis for a point of departure calculation than an approximation based on the most potent assay hit. Moreover, emergence of multiple HT probabilistic and traditional exposure modeling tools with a needed emphasis on near-field exposures (Isaacs *et al.*, 2014; Wambaugh *et al.*, 2013, 2014; Zhang *et al.*, 2014) have underscored the need for expansion and refinement of existing data sources that adequately capture chemical usage, product composition, and functional information. With efforts already underway to address these limitations, this strategy is poised to undergo key refinements that will enable its utilization as part of a Tier 1 prioritization strategy (Thomas *et al.*, 2013).

ACKNOWLEDGMENTS

The authors thank Manda Edwards, Alina Efremenko, Eric Healy, Timothy Parker, Reetu Singh, and Longlong Yang at The Hamner Institutes for Health Sciences for technical assistance provided during this project. The authors from both The Hamner Institutes for Health Sciences and USEPA thank Simcyp Limited (a Certara company) for providing access to Simcyp Simulator under a not-for-profit license agreement.

FUNDING

Funding for the research performed at The Hamner Institutes for Health Sciences, including plasma protein binding measurements, analytical chemistry analysis, computational IVIVE modeling, and PK modeling was provided by the American Chemistry Council's Long-Range Research Initiative. An equipment grant of an Agilent 6460 triple quadrupole mass spectrometer was provided by the Agilent Foundation.

SUPPLEMENTARY DATA

Supplementary data are available online at http://toxsci.oxfordjournals.org/.

REFERENCES

Adeleye, Y., Andersen, M., Clewell, R., Davies, M., Dent, M., Edwards, S., Fowler, P., Malcomber, S., Nicol, B., Scott, A., *et al.* (2015). Implementing toxicity testing in the 21st Century (TT21C): Making safety decisions using toxicity pathways, and progress in a prototype risk assessment. *Toxicol.* **332**, 102–111.

Adkison, K. K., Vaidya, S. S., Lee, D. Y., Koo, S. H., Li, L., Mehta, A. A., Gross, A. S., Polli, J. W., Humphreys, J. E., Lou, Y., *et al.* (2010). Oral sulfasalazine as a clinical BCRP probe substrate: Pharmacokinetic effects of genetic variation (C421A) and pantoprazole coadministration. *J. Pharm. Sci.* **99**, 1046–1062.

Akaike, H. (1974). A new look at the statistical model identification. *IEEE Trans. Automat. Contr.* **19**, 716–723.

Albert, K. S., Hallmark, M. R., Sakmar, E., Weidler, D. J., and Wagner, J. G. (1975). Pharmacokinetics of diphenhydramine in man. *J. Pharmacokinet. Biopharm.* **3**, 159–170.

Andree, B., Nyberg, S., Ito, H., Ginovart, N., Brunner, F., Jaquet, F., Halldin, C., and Farde, L. (1998). Positron emission tomographic analysis of dose-dependent MDL 100,907 binding to 5-hydroxytryptamine-2A receptors in the human brain. *J. Clin. Psychopharmacol.* **18**, 317–323.

Anjum, S., Swan, S. K., Lambrecht, L. J., Radwanski, E., Cutler, D. L., Affrime, M. B., and Halstenson, C. E. (1999). Pharmacokinetics of flutamide in patients with renal insufficiency. *Br. J. Clin. Pharmacol.* **47**, 43–47.

Argenti, D., Jensen, B. K., Hensel, R., Bordeaux, K., Schleimer, R., Bickel, C., and Heald, D. (2000). A mass balance study to evaluate the biotransformation and excretion of [14C]-triamcinolone acetonide following oral administration. *J. Clin. Pharmacol.* **40**, 770–780.

Arnot, J. A., Mackay, D., Webster, E., and Southwood, J. M. (2006). Screening level risk assessment model for chemical fate and effects in the environment. *Environ. Sci. Technol.* **40**, 2316–2323.

Attene-Ramos, M. S., Miller, N., Huang, R., Michael, S., Itkin, M., Kavlock, R. J., Austin, C. P., Shinn, P., Simeonov, A., Tice, R. R., *et al.* (2013). The Tox21 robotic platform for the assessment of environmental chemicals-from vision to reality. *Drug Discov. Today* **18**, 716–723.

Barter, Z. E., Bayliss, M. K., Beaune, P. H., Boobis, A. R., Carlile, D. J., Edwards, R. J., Houston, J. B., Lake, B. G., Lipscomb, J. C., Pelkonen, O. R., *et al.* (2007). Scaling factors for the extrapolation of in vivo metabolic drug clearance from in vitro data: Reaching a consensus on values of human microsomal protein and hepatocellularity per gram of liver. *Curr. Drug Metab.* **8**, 33–45.

Beaumont, K. C., Causey, A. G., Coates, P. E., and Smith, D. A. (1996). Pharmacokinetics and metabolism of zamifenacin in mouse, rat, dog and man. *Xenobiotica* **26**, 459–471.

Blyden, G. T., Greenblatt, D. J., Scavone, J. M., and Shader, R. I. (1986). Pharmacokinetics of diphenhydramine and a demethylated metabolite following intravenous and oral administration. *J. Clin. Pharmacol.* **26**, 529–533.

Bramer, S. L., Brisson, J., Corey, A. E., and Mallikaarjun, S. (1999). Effect of multiple cilostazol doses on single dose lovastatin pharmacokinetics in healthy volunteers. *Clin. Pharmacokinet.* **37**(Suppl. 2), 69–77.

Brien, J. F., Inaba, T., and Kalow, W. (1975). Comparative drug elimination in man-diphenylhydantoin and amobarbital. *Eur. J. Clin. Pharmacol.* **9**, 79–83.

Calafat, A. M. (2012). The U.S. National Health and Nutrition Examination Survey and human exposure to environmental chemicals. *Int. J. Hyg. Environ. Health* **215**, 99–101.

Cockcroft, D. W., and Gault, M. H. (1976). Prediction of creatinine clearance from serum creatinine. *Nephron* **16**, 31–41.

Cox, L. A., Popken, D., Marty, M. S., Rowlands, J. C., Patlewicz, G., Goyak, K. O., and Becker, R. A. (2014). Developing scientific confidence in HTS-derived prediction models: Lessons learned from an endocrine case study. *Regul. Toxicol. Pharmacol.* **69**, 443–450.

Critchley, J. A., Critchley, L. A., Anderson, P. J., and Tomlinson, B. (2005). Differences in the single-oral-dose pharmacokinetics and urinary excretion of paracetamol and its conjugates between Hong Kong Chinese and Caucasian subjects. *J. Clin. Pharm. Ther.* **30**, 179–184.

Davies, B., and Morris, T. (1993). Physiological parameters in laboratory animals and humans. *Pharm. Res.* **10**, 1093–1095.

Derendorf, H., Hochhaus, G., Rohatagi, S., Mollmann, H., Barth, J., Sourgens, H., and Erdmann, M. (1995). Pharmacokinetics of triamcinolone acetonide after intravenous, oral, and inhaled administration. *J. Clin. Pharmacol.* **35**, 302–305.

Dionisio, K. L., Frame, A. M., Goldsmith, M.-R., Wambaugh, J. F., Liddell, A., Cathey, T., Smith, D., Vail, J., Ernstoff, A. S., and Fantke, P. (2015). Exploring consumer exposure pathways and patterns of use for chemicals in the environment. *Toxicol. Reports* **2**, 228–237.

Dix, D. J., Houck, K. A., Martin, M. T., Richard, A. M., Setzer, R. W., and Kavlock, R. J. (2007). The ToxCast program for prioritizing toxicity testing of environmental chemicals. *Toxicol. Sci.* **95**, 5–12.

Doser, K., Guserle, R., Kramer, R., Laufer, S., and Lichtenberger, K. (1997). Bioequivalence evaluation of two flutamide preparations in healthy female subjects. *Arzneimittelforschung* **47**, 213–217.

Ferry, A., Jaillon, P., Lecocq, B., Lecocq, V., and Jozefczak, C. (1989). Pharmacokinetics and effects on exercise heart rate of PK 11195 (52028 RP), an antagonist of peripheral benzodiazepine receptors, in healthy volunteers. *Fundam. Clin. Pharmacol.* **3**, 383–392.

Gelotte, C. K., Auiler, J. F., Lynch, J. M., Temple, A. R., and Slattery, J. T. (2007). Disposition of acetaminophen at 4, 6, and 8 g/day for 3 days in healthy young adults. *Clin. Pharmacol. Ther.* **81**, 840–848.

Giles, H. G., Roberts, E. A., Orrego, H., and Sellers, E. M. (1981). Disposition of intravenous propylthiouracil. *J. Clin. Pharmacol.* **21**, 466–471.

Goldsmith, M. R., Grulke, C. M., Brooks, R. D., Transue, T. R., Tan, Y. M., Frame, A., Egeghy, P. P., Edwards, R., Chang, D. T., Tornero-Velez, R., *et al.* (2014). Development of a consumer product ingredient database for chemical exposure screening and prioritization. *Food Chem. Toxicol.* **65**, 269–279.

Gu, G. Z., Xia, H. M., Pang, Z. Q., Liu, Z. Y., Jiang, X. G., and Chen, J. (2011). Determination of sulphasalazine and its main metabolite sulphapyridine and 5-aminosalicylic acid in human plasma by liquid chromatography/tandem mass spectrometry and its application to a pharmacokinetic study. *J. Chromatogr. B Analyt. Technol. Biomed. Life Sci.* **879**, 449–456.

Hallifax, D., Foster, J. A., and Houston, J. B. (2010). Prediction of human metabolic clearance from in vitro systems: Retrospective analysis and prospective view. *Pharm. Res.* **27**, 2150–2161.

Hochhaus, G., Portner, M., Barth, J., Mollmann, H., and Rohdewald, P. (1990). Oral bioavailability of triamcinolone tablets and a triamcinolone diacetate suspension. *Pharm. Res.* **7**, 558–560.

Houck, K. A., Dix, D. J., Judson, R. S., Kavlock, R. J., Yang, J., and Berg, E. L. (2009). Profiling bioactivity of the ToxCast chemical library using BioMAP primary human cell systems. *J. Biomol. Screen* **14**, 1054–1066.

Houston, J. B., Rowland-Yeo, K., and Zanelli, U. (2012). Evaluation of the novel in vitro systems for hepatic drug clearance and assessment of their predictive utility. *Toxicol. In Vitro* **26**, 1265–1271.

Huang, R., Xia, M., Cho, M. H., Sakamuru, S., Shinn, P., Houck, K. A., Dix, D. J., Judson, R. S., Witt, K. L., Kavlock, R. J., *et al.* (2011). Chemical genomics profiling of environmental chemical modulation of human nuclear receptors. *Environ. Health Perspect.* **119**, 1142–1148.

Imai, T., and Ohura, K. (2010). The role of intestinal carboxylesterase in the oral absorption of prodrugs. *Curr. Drug Metab.* **11**, 793–805.

Isaacs, K. K., Glen, W. G., Egeghy, P., Goldsmith, M. R., Smith, L., Vallero, D., Brooks, R., Grulke, C. M., and Ozkaynak, H. (2014). SHEDS-HT: An integrated probabilistic exposure model for prioritizing exposures to chemicals with near-field and dietary sources. *Environ. Sci. Technol.* **48**, 12750–12759.

Jamei, M., Marciniak, S., Feng, K., Barnett, A., Tucker, G., and Rostami-Hodjegan, A. (2009). The Simcyp((R)) population-based ADME simulator. *Expert. Opin. Drug Metab. Toxicol.* **5**, 211–223.

Johnson, T. N., Tucker, G. T., Tanner, M. S., and Rostami-Hodjegan, A. (2005). Changes in liver volume from birth to adulthood: A meta-analysis. *Liver Transpl.* **11**, 1481–1493.

Judson, R., Richard, A., Dix, D. J., Houck, K., Martin, M., Kavlock, R., Dellarco, V., Henry, T., Holderman, T., Sayre, P., *et al.* (2009). The toxicity data landscape for environmental chemicals. *Environ. Health Perspect.* **117**, 685–695.

Judson, R. S., Houck, K. A., Kavlock, R. J., Knudsen, T. B., Martin, M. T., Mortensen, H. M., Reif, D. M., Rotroff, D. M., Shah, I., Richard, A. M., *et al.* (2010). In vitro screening of environmental chemicals for targeted testing prioritization: The ToxCast project. *Environ. Health Perspect.* **118**, 485–492.

Judson, R. S., Kavlock, R. J., Setzer, R. W., Cohen Hubal, E. A., Martin, M. T., Knudsen, T. B., Houck, K. A., Thomas, R. S., Wetmore, B. A., and Dix, D. J. (2011). Estimating toxicity-related biological pathway altering doses for high-throughput chemical risk assessment. *Chem. Res. Toxicol.* **24**, 451–462.

Kabanda, L., Lefebvre, R. A., and Remon, J. P. (1996). In-vivo evaluation in man of a hydrophilic matrix containing propylthiouracil. *J. Pharm. Pharmacol.* **48**, 1023–1026.

Kavlock, R., Chandler, K., Houck, K., Hunter, S., Judson, R., Kleinstreuer, N., Knudsen, T., Martin, M., Padilla, S., Reif, D., Richard, A., *et al.* (2012). Update on EPA's ToxCast program: Providing high throughput decision support tools for chemical risk management. *Chem. Res. Toxicol.* **25**, 1287–1302.

Kavlock, R. J., Austin, C. P., and Tice, R. R. (2009). Toxicity testing in the 21st century: Implications for human health risk assessment. *Risk Anal.* **29**, 485–487; discussion 492–497.

Kaye, B., Brearley, C. J., Cussans, N. J., Herron, M., Humphrey, M. J., and Mollatt, A. R. (1997). Formation and pharmacokinetics of the active drug candoxatrilat in mouse, rat, rabbit, dog and man following administration of the prodrug candoxatril. *Xenobiotica* **27**, 1091–1102.

Kilford, P. J., Gertz, M., Houston, J. B., and Galetin, A. (2008). Hepatocellular binding of drugs: Correction for unbound fraction in hepatocyte incubations using microsomal binding or drug lipophilicity data. *Drug Metab. Dispos.* **36**, 11941197.

Kleinstreuer, N. C., Judson, R. S., Reif, D. M., Sipes, N. S., Singh, A. V., Chandler, K. J., Dewoskin, R., Dix, D. J., Kavlock, R. J., and Knudsen, T. B. (2011). Environmental impact on vascular development predicted by high throughput screening. *Environ. Health Perspect.* **119**, 1596–1603.

Kleinstreuer, N. C., Yang, J., Berg, E. L., Knudsen, T. B., Richard, A. M., Martin, M. T., Reif, D. M., Judson, R. S., Polokoff, M., Dix, D. J., *et al.* (2014). Phenotypic screening of the ToxCast chemical library to classify toxic and therapeutic mechanisms. *Nat. Biotechnol.* **32**, 583–591.

Knight, A. W., Little, S., Houck, K., Dix, D., Judson, R., Richard, A., McCarroll, N., Akerman, G., Yang, C., Birrell, L., *et al.* (2009). Evaluation of high-throughput genotoxicity assays used in profiling the US EPA ToxCast chemicals. *Regul. Toxicol. Pharmacol.* **55**, 188–199.

Knudsen, T. B., Houck, K. A., Sipes, N. S., Singh, A. V., Judson, R. S., Martin, M. T., Weissman, A., Kleinstreuer, N. C., Mortensen, H. M., Reif, D. M., *et al.* (2011). Activity profiles of 309 ToxCast chemicals evaluated across 292 biochemical targets. *Toxicology* **282**, 1–15.

Kobayashi, Y., Fukami, T., Shimizu, M., Nakajima, M., and Yokoi, T. (2012). Contributions of arylacetamide deacetylase and carboxylesterase 2 to flutamide hydrolysis in human liver. *Drug Metab. Dispos.* **40**, 1080–1084.

Kothare, P. A., Linnebjerg, H., Skrivanek, Z., Reddy, S., Mace, K., Pena, A., Han, J., Fineman, M., and Mitchell, M. (2007). Exenatide effects on statin pharmacokinetics and lipid response. *Int. J. Clin. Pharmacol. Ther.* **45**, 114–120.

Krewski, D., Westphal, M., Andersen, M. E., Paoli, G. M., Chiu, W. A., Al-Zoughool, M., Croteau, M. C., Burgoon, L. D., and Cote, I. (2014). A framework for the next generation of risk science. *Environ. Health Perspect.* **122**, 796–805.

Lamiable, D., Vistelle, R., Trenque, T., Fay, R., Millart, H., and Choisy, H. (1993). Sensitive high-performance liquid chromatographic method for the determination of coumarin in plasma. *J. Chromatogr.* **620**, 273–277.

Landesmann, B., Mennecozzi, M., Berggren, E., and Whelan, M. (2013). Adverse outcome pathway-based screening strategies for an animal-free safety assessment of chemicals. *Altern. Lab. Anim.* **41**, 461–471.

Li, A. P., Lu, C., Brent, J. A., Pham, C., Fackett, A., Ruegg, C. E., and Silber, P. M. (1999). Cryopreserved human hepatocytes: Characterization of drug-metabolizing enzyme activities and applications in higher throughput screening assays for hepatotoxicity, metabolic stability, and drug-drug interaction potential. *Chem. Biol. Interact.* **121**, 17–35.

Lindemalm, S., Savic, R. M., Karlsson, M. O., Juliusson, G., Liliemark, J., and Albertioni, F. (2005). Application of population pharmacokinetics to cladribine. *BMC Pharmacol.* **5**, 4.

Luna, B. G., Scavone, J. M., and Greenblatt, D. J. (1989). Doxylamine and diphenhydramine pharmacokinetics in women on low-dose estrogen oral contraceptives. *J. Clin. Pharmacol.* **29**, 257–260.

Ma, J. J., Liu, C. G., Li, J. H., Cao, X. M., Sun, S. L., and Yao, X. (2009). Effects of NAT2 polymorphism on SASP pharmacokinetics in Chinese population. *Clin. Chim. Acta* **407**, 30–35.

Martin, M. T., Dix, D. J., Judson, R. S., Kavlock, R. J., Reif, D. M., Richard, A. M., Rotroff, D. M., Romanov, S., Medvedev, A., Poltoratskaya, N., *et al.* (2010). Impact of environmental chemicals on key transcription regulators and correlation to toxicity end points within EPA's ToxCast program. *Chem. Res. Toxicol.* **23**, 578–590.

Martin, M. T., Knudsen, T. B., Reif, D. M., Houck, K. A., Judson, R. S., Kavlock, R. J., and Dix, D. J. (2011). Predictive model of rat reproductive toxicity from ToxCast high throughput screening. *Biol. Reprod.* **85**, 327–339.

McMullen, P. D., Bhattacharya, S., Woods, C.G., Sun, B., Yarborough, K., Ross, S.M., Miller, M.E., McBride, M.T., LeCluyse, E.L., Clewell, R.A., *et al.* (2014). A map of the PPARα transcription regulatory network for primary human hepatocytes. *Chem. Biol. Interact.* **209**, 14–24.

Mennecozzi, M., Landesmann, B., Harris, G.A., Liska, R., and Whelan, M. (2012). Hepatotoxicity screening taking a mode-of-action approach using HepaRG cells and HCA. *ALTEX* **1**, 193–204.

Mielke, H., Abraham, K., Gotz, M., Vieth, B., Lampen, A., Luch, A., and Gundert-Remy, U. (2011). Physiologically based toxicokinetic modelling as a tool to assess target organ toxicity in route-to-route extrapolation-the case of coumarin. *Toxicol. Lett.* **202**, 100–110.

Mignini, F., Tomassoni, D., Streccioni, V., Traini, E., and Amenta, F. (2008). Pharmacokinetics and bioequivalence study of two tablet formulations of lovastatin in healthy volunteers. *Clin. Exp. Hypertens* **30**, 95–108.

Morgan, J. A., and Tatar, J. F. (1972). Calculation of the residual sum of squares for all possible regressions. *Technometrics* **14**, 317–325.

Nolan, R. J., Freshour, N. L., Kastl, P. E., and Saunders, J. H. (1984). Pharmacokinetics of picloram in male volunteers. *Toxicol. Appl. Pharmacol.* **76**, 264–269.

NRC. (2007). *Toxicity Testing in the 21st Century: A Vision and a Strategy*. National Research Council of the National Academies, Washington, D.C.

Pastrello, C., Pasini, E., Kotlyar, M., Otasek, D., Wong, S., Sangrar, W., Rahmati, S., and Jurisica, I. (2014). Integration, visualization and analysis of human interactome. *Biochem. Biophys. Res. Commun.* **445**, 757–773.

Pelkonen, O., Turpeinen, M., Hakkola, J., Abass, K., Pasanen, M., Raunio, H., and Vahakangas, K. (2013). Preservation, induction or incorporation of metabolism into the in vitro cellular system - views to current opportunities and limitations. *Toxicol. In Vitro* **27**, 1578–1583.

Pleil, J. D., Stiegel, M. A., Madden, M. C., and Sobus, J. R. (2011). Heat map visualization of complex environmental and biomarker measurements. *Chemosphere* **84**, 716–723.

Plyte, S. E., Hughes, K., Nikolakaki, E., Pulverer, B. J., and Woodgett, J. R. (1992). Glycogen synthase kinase-3: Functions in oncogenesis and development. *Biochim. Biophys. Acta* **1114**, 147–162.

Radwanski, E., Perentesis, G., Symchowicz, S., and Zampaglione, N. (1989). Single and multiple dose pharmacokinetic evaluation of flutamide in normal geriatric volunteers. *J. Clin. Pharmacol.* **29**, 554–558.

Reif, D. M., Sypa, M., Lock, E. F., Wright, F. A., Wilson, A., Cathey, T., Judson, R. R., and Rusyn, I. (2013). ToxPi GUI: An interactive visualization tool for transparent integration of data from diverse sources of evidence. *Bioinformatics* **29**, 402–403.

Rosenbaum, R. K., Bachmann, T. M., Swirsky Gold, L., Huijbregts, M. A. J., Jolliet, O., Juraske, R., Koehler, A., Larsen, H.F., MacLeod, M., Margni, M., *et al.* (2008). USEtox - The UNEP-SETAC toxicity model: Recommended characterization factors for human toxicity and freshwater ecotoxicity in life cycle impact assessment. . Int. J.Life Cycle Assess. **13**, 532–546.

Rostami-Hodjegan, A., Shiran, M. R., Tucker, G. T., Conway, B. R., Irwin, W. J., Shaw, L. R., and Grattan, T. J. (2002). A new rapidly absorbed paracetamol tablet containing sodium bicarbonate. II. Dissolution studies and in vitro/in vivo correlation. *Drug Dev. Ind. Pharm.* **28**, 533–543.

Rotroff, D. M., Beam, A. L., Dix, D. J., Farmer, A., Freeman, K. M., Houck, K. A., Judson, R. S., LeCluyse, E. L., Martin, M. T., Reif, D. M., *et al.* (2010a). Xenobiotic-metabolizing enzyme and transporter gene expression in primary cultures of human hepatocytes modulated by ToxCast chemicals. *J. Toxicol. Environ. Health B.- Crit. Rev.* **13**, 329–346.

Rotroff, D. M., Dix, D. J., Houck, K. A., Kavlock, R. J., Knudsen, T. B., Martin, M. T., Reif, D. M., Richard, A. M., Sipes, N. S., Abassi, Y. A., *et al.* (2013). Real-time growth kinetics measuring hormone mimicry for ToxCast chemicals in T-47D human ductal carcinoma cells. *Chem. Res. Toxicol.* **26**, 1097–1107.

Rotroff, D. M., Wetmore, B. A., Dix, D. J., Ferguson, S. S., Clewell, H. J., Houck, K. A., Lecluyse, E. L., Andersen, M. E., Judson, R. S., Smith, C. M., *et al.* (2010b). Incorporating human dosimetry and exposure into high-throughput in vitro toxicity screening. *Toxicol. Sci.* **117**, 348–358.

Sipes, N. S., Martin, M. T., Kothiya, P., Reif, D. M., Judson, R. S., Richard, A. M., Houck, K. A., Dix, D. J., Kavlock, R. J., and Knudsen, T. B. (2013). Profiling 976 ToxCast chemicals across 331 enzymatic and receptor signaling assays. *Chem. Res. Toxicol.* **26**, 878–895.

Sipes, N. S., Martin, M. T., Reif, D. M., Kleinstreuer, N. C., Judson, R. S., Singh, A. V., Chandler, K. J., Dix, D. J., Kavlock, R. J., and Knudsen, T. B. (2011). Predictive models of prenatal developmental toxicity from ToxCast high-throughput screening data. *Toxicol. Sci.* **124**, 109–127.

Smith, C. M., Nolan, C. K., Edwards, M. A., Hatfield, J. B., Stewart, T. W., Ferguson, S. S., Lecluyse, E. L., and Sahi, J. (2012). A comprehensive evaluation of metabolic activity and intrinsic clearance in suspensions and monolayer cultures of cryopreserved primary human hepatocytes. *J. Pharm. Sci.* **101**, 3989–4002.

Tan, Y. M., Liao, K. H., and Clewell, H. J., III. (2007). Reverse dosimetry: Interpreting trihalomethanes biomonitoring data using physiologically based pharmacokinetic modeling. *J. Expo. Sci. Environ. Epidemiol.* **17**, 591–603.

Thomas, R. S., Black, M. B., Li, L., Healy, E., Chu, T. M., Bao, W., Andersen, M. E., and Wolfinger, R. D. (2012). A comprehensive statistical analysis of predicting in vivo hazard using high-throughput in vitro screening. *Toxicol. Sci.* **128**, 398–417.

Thomas, R. S., Philbert, M. A., Auerbach, S. S., Wetmore, B. A., Devito, M. J., Cote, I., Rowlands, J. C., Whelan, M. P., Hays, S. M., Andersen, M. E., *et al.* (2013). Incorporating new technologies into toxicity testing and risk assessment: Moving from 21st century vision to a data-driven framework. *Toxicol. Sci.* **136**, 4–18.

Toothaker, R. D., Barker, S. H., Gillen, M. V., Helsinger, S. A., Kindberg, C. G., Hunt, T. L., and Powell, J. H. (2000). Absence of pharmacokinetic interaction between orally co-administered naproxen sodium and diphenhydramine hydrochloride. *Biopharm. Drug Dispos.* **21**, 229–233.

Tukey, J. W. (1977). *Exploratory Data Analysis*. Addison-Wesley, Reading, MA.

Wambaugh, J. F., Setzer, R. W., Reif, D. M., Gangwal, S., Mitchell-Blackwood, J., Arnot, J. A., Joliet, O., Frame, A., Rabinowitz, J., Knudsen, T. B., *et al.* (2013). High-throughput models for exposure-based chemical prioritization in the ExpoCast project. *Environ. Sci. Technol.* **47**, 8479–8488.

Wambaugh, J. F., Wang, A., Dionisio, K. L., Frame, A., Egeghy, P., Judson, R., and Setzer, R. W. (2014). High throughput heuristics for prioritizing human exposure to environmental chemicals. *Environ. Sci. Technol.* **48**, 12760–12767.

Waters, N. J., Jones, R., Williams, G., and Sohal, B. (2008). Validation of a rapid equilibrium dialysis approach for the measurement of plasma protein binding. *J. Pharm. Sci.* **97**, 4586–4595.

Wetmore, B.A. (2015). Quantitative *in vitro*-to-*in vivo* extrapolation in a high-throughput environment. *Toxicology* **332**, 94–101.

Wetmore, B. A., Wambaugh, J. F., Ferguson, S. S., Li, L., Clewell, H. J., III, Judson, R. S., Freeman, K., Bao, W., Sochaski, M. A., Chu, T. M., *et al.* (2013). Relative impact of incorporating pharmacokinetics on predicting in vivo hazard and mode of action from high-throughput in vitro toxicity assays. *Toxicol. Sci.* **132**, 327–346.

Wetmore, B. A., Wambaugh, J. F., Ferguson, S. S., Sochaski, M. A., Rotroff, D. M., Freeman, K., Clewell, H. J., III, Dix, D. J., Andersen, M. E., Houck, K. A., *et al.* (2012). Integration of

dosimetry, exposure, and high-throughput screening data in chemical toxicity assessment. *Toxicol. Sci.* **125**, 157–174.

Whitlam, J. B., and Brown, K. F. (1981). Ultrafiltration in serum protein binding determinations. *J. Pharm. Sci.* **70**, 146–150.

Yasui-Furukori, N., Kondo, T., Mihara, K., Suzuki, A., Inoue, Y., De Vries, R., and Kaneko, S. (2002). Lack of correlation between the steady-state plasma concentrations of haloperidol and risperidone. *J. Clin. Pharmacol.* **42**, 1083–1088.

Zhang, X., Arnot, J. A., and Wania, F. (2014). Model for screening-level assessment of near-field human exposure to neutral organic chemicals released indoors. *Environ. Sci. Technol.* **48**, 12312–12319.